THE IMPORTANCE OF DECOMPOSING NIGHTTIME LIGHT IMAGERY FOR POST-EARTHQUAKE ASSESSMENT AND RECOVERY

I. Alisjahbana[(1)], A. Kiremidjian[(2)]

[(1)] *PhD Student, Department of Civil & Environmental Engineering, Stanford University, USA, alisjahbana@stanford.edu*
[(2)] *Professor, Department of Civil & Environmental Engineering, Stanford University, USA, ask@stanford.edu*

Abstract

Nighttime light imagery has been shown to be useful in analyzing the impacts to human activities after major earthquakes. In this study, we used the National Polar-orbiting Partnership Visible Infrared Imaging Radiometer Suite (NPP-VIIRS) Day/Night Band (DNB) monthly composites to assess the impact and subsequent recovery period of major earthquakes. We demonstrate the importance of decomposing the nighttime light time series to remove changes in nighttime light imagery that are not related to the effects of the earthquake. For each month, the NPP-VIIRS data are calculated into a single value of total radiance. We then decompose the nighttime light time series data into trend and seasonal components and use a Bayesian estimator to model the time series data to detect underlying changes in the components. This study was performed on 3 past earthquake events in Indonesia: the 2013 Aceh earthquake, the 2016 Aceh earthquake and the 2018 Sulawesi earthquake. From these analyses, change points were detected in the trend component of the time series data for all three case studies, showing that nighttime light imagery can indeed be used to monitor the effects of the earthquake, as long as it is separated into the trend and seasonal component. Our analyses show that though nighttime light imagery can be used to assess post-earthquake activities, cloud cover is a major limitation and that nighttime light imagery is suited to more urban areas rather than rural areas.

Keywords: community recovery; nighttime light imagery; post-earthquake assessment; time-series decomposition; changepoint detection

1. Introduction

It is well recognized that earthquakes cause thousands of causalities, destroy many buildings and result in millions of dollars of loss every year. The process of recovery after an earthquake is often long and very complex because of the various factors and stakeholders that are involved. After a major event, large amount of time, effort and resources are spent by the government, international organizations and other agencies in order to reach specific recovery goals, whether it is to restore basic services as fast as possible, rebuild the communities or restore livelihoods [1]. As a result, the recovery of a region needs to be monitored in order to assess the progress being done and address issues more rapidly.

Traditional methods of damage assessments and recovery monitoring rely on ground-based surveys and field assessments which involves dispatching experts to the field to manually inspect buildings and other infrastructure individually. Though it is still the most relied method of assessment, this method is often time consuming to apply across large geographic regions, highly subjective prone to inconsistencies in data quality and very costly [2]. As a result, remote sensing has increasingly played a major role in assessing the impacts of earthquakes.

The use of remote sensing in post-disaster and recovery assessments have been well recognized [3]–[5]. For example, very high resolution satellite imagery has been used to rapidly detect damaged areas after earthquakes [6]–[9]. Other sources of remote sensing data such as Synthetic Aperture Radar (SAR) [6], [10]–[13], LiDAR [14], [15] and UAV imagery [16]–[19] have also been used.

Though remote sensing data such as optical satellite imagery and SAR enable the detection of structural damage due to earthquakes and is able to monitor the process of reconstruction in the subsequent recovery phase, it does not provide direct information on human activities. Nighttime light (NTL) imagery is able to provide a new perspective on human activities, and has been often used to track socioeconomic factors [20], urbanization [21]–[23], electricity [24], [25] and even armed conflicts [26], [27]. Studies have shown that NTL is also useful to assess the impacts of major disasters to communities [1], [28]–[31]. Because natural disasters can cause damage to buildings and cause power outages, Brown et al. [1] used NTL as a proxy to monitor the recovery of a community after the 2004 Sumatra Earthquake.

The two commonly used data sources are the Defense Meteorological Satellite Program's Operational Line Scan System (DMSP-OLS) and the Visible Infrared Imaging Radiometer Suite (VIIRS) Day-Night Band (DNB) [32]. The major advantage of the DMSP-OLS is the wide temporal coverage, with data dating back to the 1970s, making it advantageous to analyze disasters that happened decades ago. Cao et al. [33] and Li et al. [28] used DMSP-OLS data to monitor the reconstruction for the 2008 Wenchuan earthquake. Brown et al. [1], [2] also used DMSP-OLS data to monitor the recovery after the 2004 Sumatra earthquake. However, major limitations of DMSP-OLS include its coarse radiometric accuracy, low spatial resolution and lack of onboard calibration [34], making it hard to analyze the imagery over a period of time. The newer NPP-VIIRS DNB overcomes most of DMSP-OLS's limitations. In addition to higher radiometric accuracy, it has a higher dynamic range and has a higher resolution [35], making it more suitable for disaster monitoring. For example, Zhao et al. [29] used NPP-VIIRS DNB to assess the impact of three types of natural disasters and showed that they are useful for detecting damages and power outages caused by earthquake, storm and flood events. Fan et al. [30] used NPP-VIIRS DNB to rapidly identify earthquake damage after several earthquakes, showing that the accuracies increase with greater earthquake intensities.

Though there have been many studies on using the NPP-VIIRS DNB data for rapid post-disaster assessment, few researches have used the NPP-VIIRS DNB in monitoring the longer-term recovery period, partly due to its limited archive, only dating back to 2011. However, for the purposes of monitoring regions over long periods of time, studies have shown that time series data usually contains a trend and a cycle component that must be separated in order to accurately monitor the region [36]. Previous work that tracks changes using pre- and post-earthquake NTL images found that NTL typically decreases after major events, but they did not take into consideration the differences caused by the cyclic component, such as that due to the seasonal effects. This is an important consideration to take into account as the changes that are seen from the imagery can be a result of other external factors, and not only as a result of the earthquake.

This paper analyzes the change in nighttime light using NPP-VIIRS DNB monthly composite images to monitor the impact and subsequent recovery of a region due to earthquakes. Specifically, we demonstrate the importance of decomposing the NTL time series to remove changes in the NTL that are not related to the effects of the earthquake by using a Bayesian estimator to model the time series data and detect underlying changes in the components. We also analyze the usefulness and limitations of using NPP-VIIRS DNB monthly data for monitoring recovery of regions.

2. Materials and Methods

2.1 Event Selection

Because the NPP-VIIRS DNB data are only available since May 2012 [37], we selected earthquakes that occur after this date. As a result, we selected 3 past earthquakes that happened in Indonesia. The earthquakes that were chosen are those that caused significant damage to the region. The quality of the available imagery was also taken into consideration. To be able to see the trend of NTL over a period of time, we chose earthquakes that occurred recently as well as those that occurred several years ago. Table 1 lists the basic information of the selected earthquakes.

Table 1 – Selected earthquakes for the study

Event	Location	Date	Magnitude	Aftermath
2018 Sulawesi earthquake	Palu, Sulawesi, Indonesia	28 September 2018	7.5 Mw	Followed by tsunami and multiple liquefaction. Over 4,000 casualties, 10,000 injuries and over 70,000 damaged houses
2016 Aceh earthquake	Pidie Jaya, Aceh, Indonesia	7 December 2016	6.5 Mw	104 casualties, over 1,000 people injured, and hundreds of damaged houses
2013 Aceh earthquake	Bener Meriah, Aceh, Indonesia	2 July 2013	6.1 Mw	35 casualties, and over 4,300 homes damaged or destroyed

The 2018 Sulawesi earthquake was a 7.5 Mw event that occurred on 28 September 2018 with an epicenter in the Donggala Regency, Central Sulawesi, Indonesia. Similar to the 2016 Aceh earthquake, it was considered a large and shallow event but was preceded with a sequence of foreshocks. It was also followed by a tsunami that caused more than 4000 casualties as well as widespread damage to the area, especially to the capital city of Central Sulawesi, Palu [38]. The earthquake also caused major soil liquefaction in the region, which led to the deaths of hundreds more people and submerged hundreds of buildings [39].

The 2016 Aceh earthquake was a 6.5 Mw event that occurred on 7 December in Pidie Jaya, within the Aceh province of Indonesia. This earthquake killed over 100 people, injured at least 1,000 people, and caused massive power outages as telephone poles and electrical poles tumbled. It was stated that approximately 30% of the area of Pidie Jaya was severely affected by the quake [40].

The 2013 Aceh earthquake was a 6.1 Mw event that struck the Indonesian island of Sumatra on 2 July 2013. The Bener Meriah and Central Aceh districts were hardest hit by the quake with thousands of homes damaged or destroyed. Millions of dollars were allocated for emergency relief efforts [41].

2.2 Data

The NPP-VIIRS data that are utilized for this study is the Version 1 suite of average radiance composite images that are publicly available for free from [37]. These images are monthly composites, which means they are averaged over daily images during that particular month. Values are given in the amount of radiance, with a range from 3 x 10^{-9} W cm^{-2} sr^{-1} to 0.02 W cm^{-2} sr^{-}1. The NPP-VIIRS images have been filtered to exclude pixels that are impacted by external factors such as clouds, stray lights, lightning and lunar illumination. However, these images have not been filtered for temporal lights that might originate from fires, Aurora, and flaring gas. For regions that are often lighted by oil wells, a masking of the area would be ideal [42]. However, given that the regions of interest are not in proximity of oil bases, we did not do any additional preprocessing for flaring lights.

A total of 45 images were download for the 2013 Aceh earthquake between January 2013 and September 2016; 54 images for the 2016 Aceh earthquake between January 2015 and June 2019, and a total of 43 images were downloaded for the 2018 Sulawesi Earthquake between December 2015 to June 2019. Figure 1 shows the range of images that are used in this study with the corresponding earthquake event times. The range of images chosen were related to the availability of data. For example, considering NPP-VIIRS images are only available since June 2012 and the presence of cloud cover, only images from January 2013 onwards are able to be obtained for the 2013 Aceh earthquake.

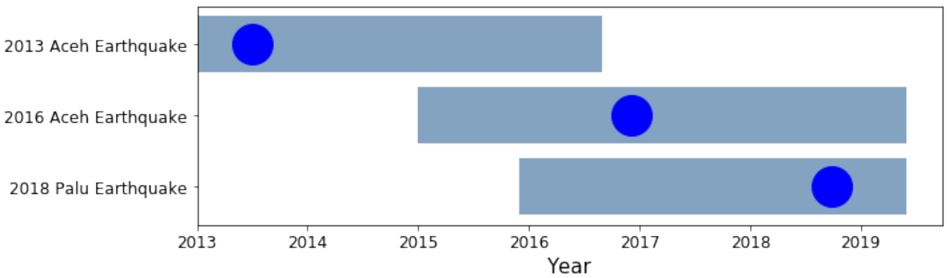

Fig. 1 – Range of images used for each earthquake event (grey bar) with the corresponding earthquake event date (blue marker)

In addition to the NTL images, administrative boundary data were obtained from OpenStreetMap (OSM) [43]. Figure 2 shows the NPP-VIIRS image for Palu in September 2018 with the administrative boundary.

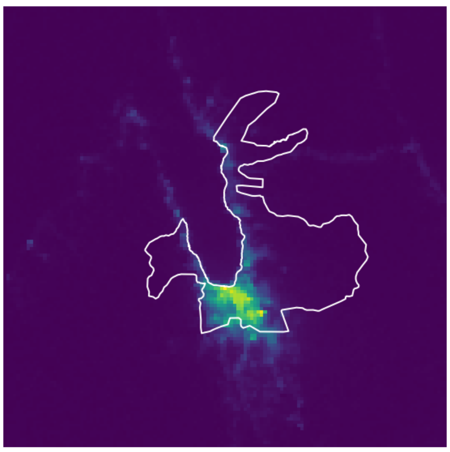

Fig. 2 – NPP-VIIRS image for Palu in September 2018 overlaid with the administrative boundary from OpenStreetMap (OSM)

2.3 Methods

All the raw images obtained from VIIRS were first preprocessed in order to account for missing pixels and cloud coverage. The total nighttime lights were then calculated from the processed images, before performing change-point detection on the time series.

2.3.1 Data Preprocessing

Ideally, to obtain a complete and accurate time series of the NTL in each region, we want the images to have no missing values. However, in reality, there are missing values for some months due to cloud cover, which has been determined using the VIIRS Cloud Mask product (VCM). By inspecting each image, we identified months that have low cloud cover (i.e. less than 15% of the total number of pixels in the image) and interpolated the missing pixels based on a simple method of inverse distance weighted (IDW) interpolation [44]. IDW assumes that pixels that are closer to one another are more similar to those that are farther apart, which can be applied to nighttime lights. For each missing pixel, a four-direction conic search is done to find values to interpolate. The missing pixels can be calculated using the following equation:

$$R = \frac{\sum_{i=1}^{n}(\frac{R_i}{d_i})}{\sum_{i=1}^{n}(\frac{1}{d_i})} \tag{1}$$

where R denotes the radiance of the pixel to interpolate, n denotes the number of pixels that are available within the maximum search radius, R_i denotes the radiance value of pixels to interpolate from, and d denotes the distance to the missing pixel. Results from the IDW interpolation for the Palu region on March 2019 can be seen in Figure 3.

It is recognized that the interpolation method would result in errors in the nighttime light values. Unfortunately, it is extremely difficult to quantitatively verify the interpolated values because the ground truth data are also unknown [44]. If reference data such as that obtained from electricity providers are available for the time span studied, it would perhaps be possible to compare the interpolated values with the reference data. However, it was not possible to obtain such information for the case studies in this paper, and therefore only visual assessment was performed on the interpolation results. This was done by comparing the interpolated results with the building densities of the region.

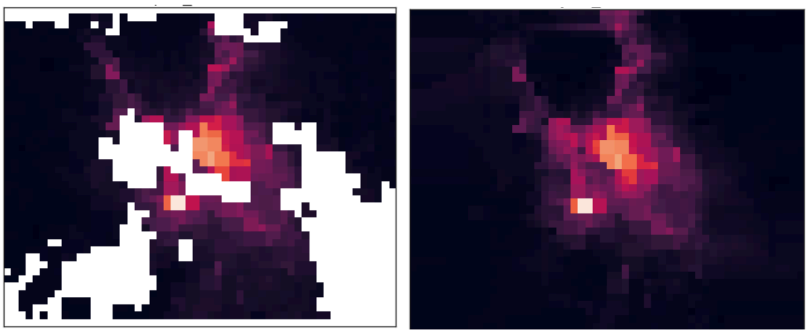

Fig. 3 – (left) Original NPP-VIIRS image with missing pixels because of cloud cover and (right) processed image by IDW interpolation for Palu region in March 2019.

For months that were identified to have a higher cloud cover percentage (i.e. more than 15% of the total number of pixels in the image), we interpolated those months by averaging the data from two adjacent months, similar to what was done in [42]. The missing month can be calculated using the following equation:

$$R_i^t = \frac{R_i^{t-1} + R_i^{t+1}}{2} \tag{2}$$

where $R_i(t)$, $R_i(t-1)$, $R_i(t+1)$ denotes the radiance values of the i-th pixel at time t, $(t-1)$ and $(t+1)$ respectively.

For images that had two consecutive months with more than 15% of cloud cover, a simple linear interpolation was done. Images that had more than two consecutive missing months were discarded.

2.3.2 Calculation of Total Nighttime Light

After processing the images for missing pixels due to cloud cover, the total nighttime light values were calculated for the region of interest. The administrative boundaries that were obtained from OSM is used to extract the pixels that fall within the boundary. The total nighttime light (R_{total}) value of the region can be calculated using the following equation:

$$R_{total} = \sum_{i=1}^{n} R_i u_i \tag{3}$$

where R_i denotes the radiance value of the i-th pixel and u_i is an indicator value with 1 if the pixel i is inside the administrative boundary and 0 otherwise. A time series of the total nighttime light can then be calculated for each region.

2.3.2 Change-Point Detection

Time series data are often described as the sum of two components: seasonal and trend signal. A third component, abrupt changes, is intrinsically embedded within the two components. This decomposition can be written as follows:

$$R_{total}(t_i) = R_S(t_i) + R_T(t_i) + \epsilon \tag{4}$$

In this study, A Bayesian Estimator of Abrupt change, Seasonal change and Trend (BEAST) that was first introduced in [36] is used to model the seasonal and trend signals and subsequently detect the abrupt change of the total nighttime light time series. In the BEAST model, the time series data are represented as a linear combination of multiple functions that decomposes the time series data into multiple trend components and seasonal components (Figure 4). The number of functions and parameters for each function that are used to represent the raw time series data are determined using a reverse-jump Markov Chain Monte Carlo (RJ-MCMC) method. More details on the BEAST formulation is available in [36].

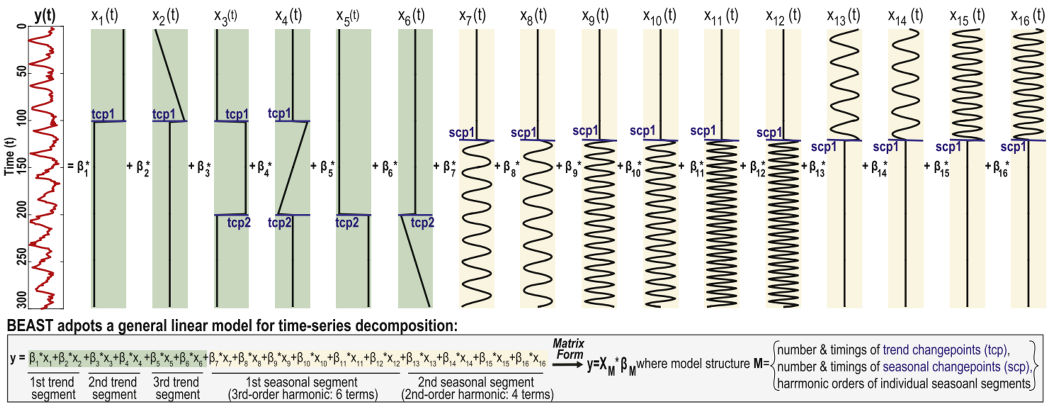

Fig. 4 – BEAST time series decomposition (obtained from [36])

The R package Rbeast was used to implement the model. The parameters used for the RJ-MCMC followed those that were recommended in [45]. In addition to decomposing the time series data into trend and seasonal signals, the BEAST method detects the changepoint and quantifies how likely each point of time is a change point.

3. Results and Discussion

3.1 2018 Sulawesi Earthquake

The nighttime light time series for the Palu region can be seen in Figure. 5. There is clearly a significant drop in the total nighttime light radiance value during the month of the 2018 Sulawesi earthquake. However, it can be seen that there are multiple other drops in values over the period of time of interest. For example, there was a significant value decrease in total nighttime light value in April 2017 (201704) that is actually more significant than the value decrease from the earthquake itself. Furthermore, though the total nighttime light value increases after the earthquake, there are additional drops in values such as that in January 2019 (201901) and June 2019 (201906). This highlights the fact that though nighttime light imagery can detect changes due to the earthquake, there are many other factors that can cause the increase and decrease of values over time, making it difficult to monitor the recovery period after the earthquake purely based on NTL.

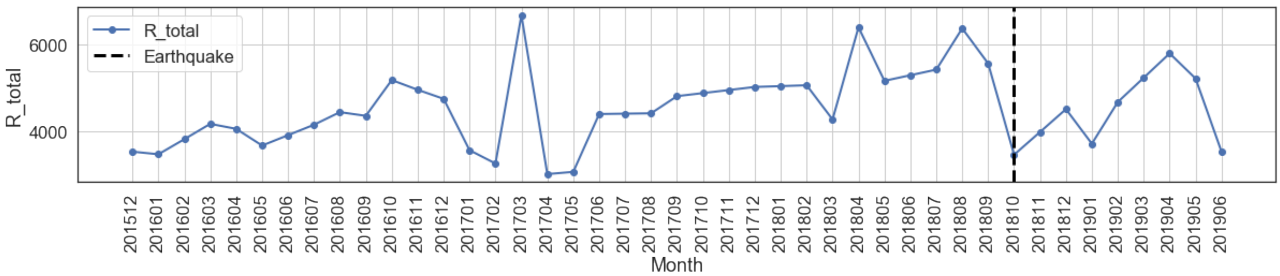

Fig. 5 – Nighttime light time series for Palu Region with the corresponding month of the 2018 Sulawesi earthquake

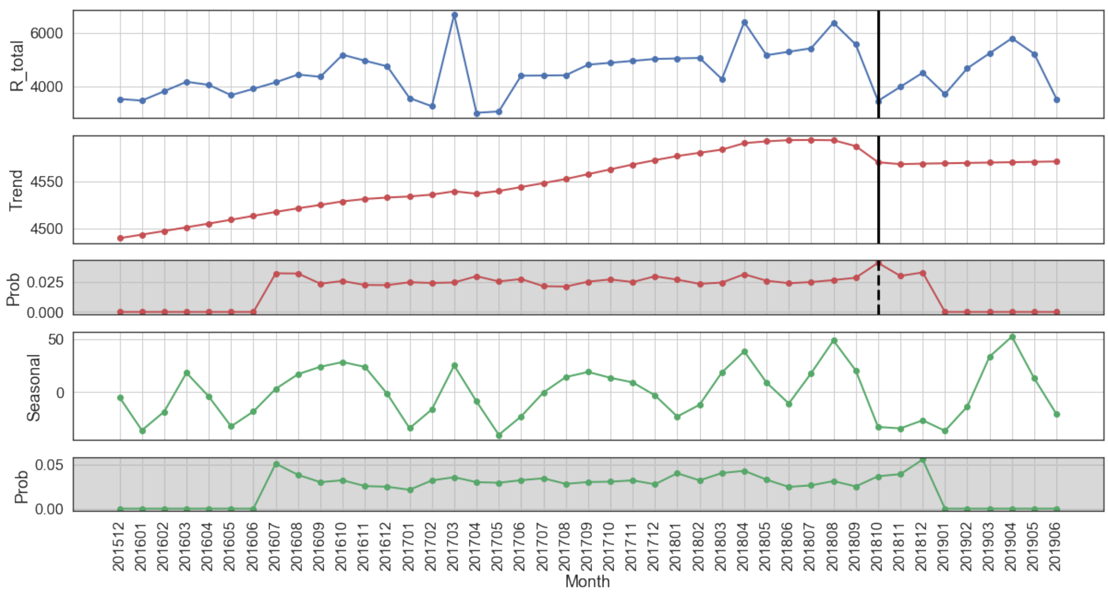

Fig. 6– BEAST time series decomposition and change detection for the Palu region corresponding to the 2018 Sulawesi earthquake

We then decomposed the timeseries data into a trend and seasonal component by fitting it into the BEAST model (Figure 6). By decomposing the time series data, it can be seen clearly that the Palu region has a linearly increasing trend component, which can be attributed to the growth and urbanization of the region itself. The BEAST model was able to detect a changepoint in the nighttime light trend in October 2018, which corresponds to the month after the earthquake happened (September 2018). A drop was observed after the month of the earthquake, and since then, the trend is constant. This might point to the fact that the city has not recovered since the earthquake. By removing the noise and underlying seasonal component, the effects of the earthquake to the nighttime light is clear through the trend component of the time series.

3.2 2016 Aceh Earthquake

The total nighttime light time series for the Pidie Jaya region can be seen in Figure 7. Due to cloud cover, there were multiple months in which there were too many missing pixels. As a result, we discarded the images from April 2018 to November 2018. Similar to the 2018 Sulawesi earthquake, there are multiple increases and drops in total nighttime light radiance over the period of time of interest. Though there was a drop in total nighttime light radiance during the month of the earthquake, it is quite unclear whether that is attributed to the earthquake itself or whether that is a result of other external factors given that several months prior to the earthquake, the total nighttime light radiance has slowly decreased too.

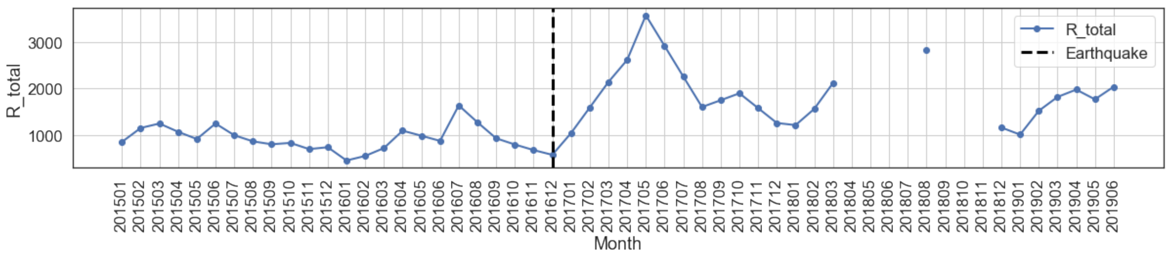

Fig. 7 – Nighttime light time series for Pidie Jaya Region with the corresponding month to the 2016 Aceh earthquake

Results from the BEAST model can be seen in Figure 8. BEAST is able to take in time series data that are with missing values by fitting a nonlinear curve to the data with gaps [36]. Similar to the 2018 Sulawesi earthquake, the algorithm was able to accurately detect a change point in the trend signal during the month of the earthquake (December 2016).

It is interesting to note however, that after that particular month, the total nighttime light radiance value actually increases until May 2017 and decreases sharply again in June 2017. This is seen from another change point that was detected by the algorithm in June 2017. We have looked through external sources such as news, and local government, but was unable to pinpoint the cause of this change of total nighttime light. One possible explanation is that the area in general does not have too much light during normal times. However, after the earthquake occurred, reconstruction and recovery activity increases, which in turn causes the total nighttime light to increase. Given that Pidie Jaya is a small region mostly covered by forest, this is similar to what was observed in the study done by Zhao et al. [29], where they show that in mountainous areas or small villages, the nighttime light actually increases after the earthquake and not vice versa.

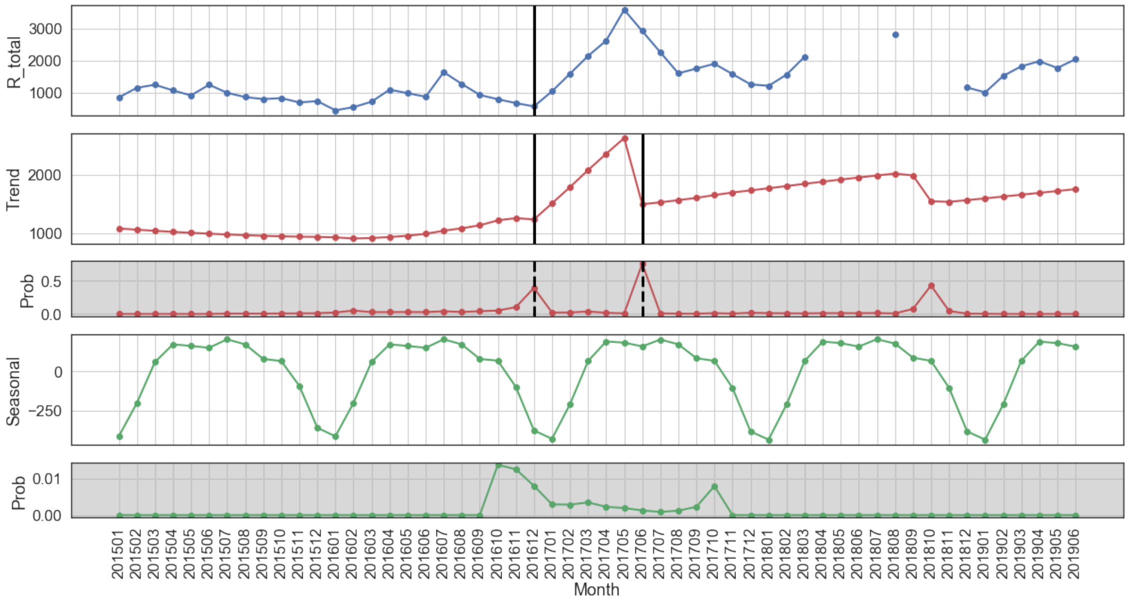

Fig. 8 – BEAST time series decomposition for the Pidie Jaya region with the detected change corresponding to the 2016 Aceh earthquake

3.1 2013 Aceh Earthquake

Finally, we performed the analysis on one of the earlier earthquakes that is within the time period of the NPP-VIIRS DNB data acquisition. The total nighttime light time series for the Bener Meriah region can be seen in Figure 9. Similar to the Palu and Pidie Jaya region, the total nighttime light time series has a lot of variance, and it isn't very clear whether the 2013 earthquake had some effect to the nighttime light value of the region. Furthermore, it is difficult to monitor whether the earthquake had any lasting effect to the region.

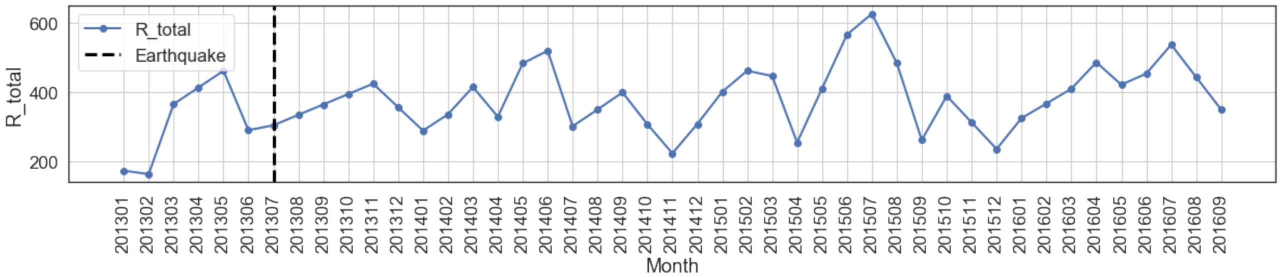

Fig. 9 – Nighttime light time series for Bener Meriah Region with the corresponding month to the 2013 Aceh earthquake

Results of the time series decomposition for the 2013 Aceh earthquake can be seen in Figure 10. The BEAST algorithm was again able to quantitatively detect a change point in the time series that corresponds to the earthquake event in June 2013. However, when looking at the trend component of the total nighttime light time series, it is interesting to note that the earthquake did not change the trajectory of the time series. This is different to what was observed in the 2018 Sulawesi earthquake and the 2016 Aceh earthquake. This can be attributed to the fact that the damage caused by the earthquake was not as devastating as the other two earthquakes.

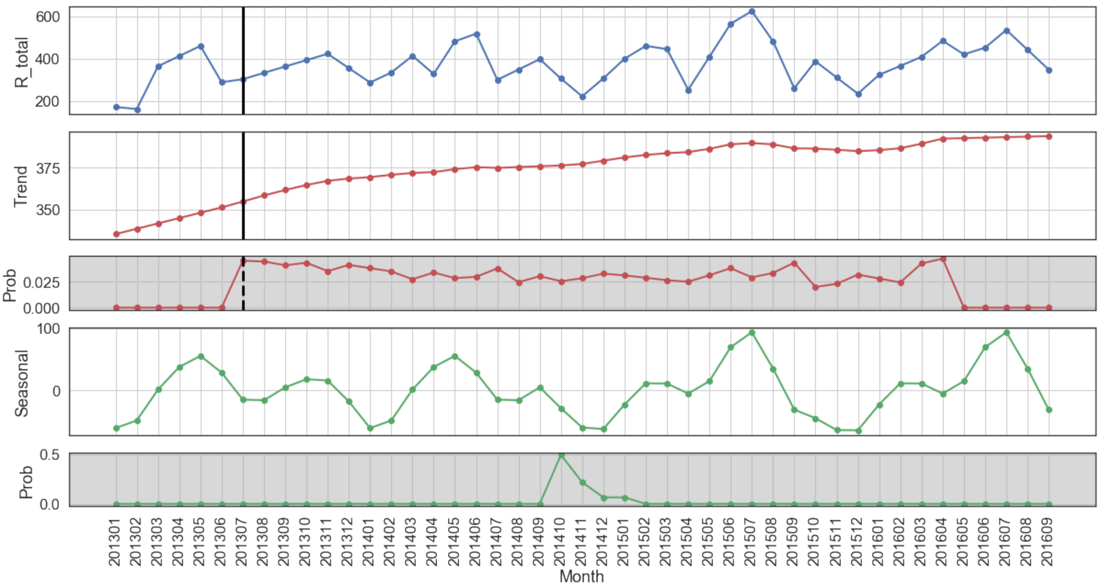

Fig. 10 – BEAST time series decomposition for the Bener Meriah region with the detected change corresponding to the 2013 Aceh earthquake

4. Conclusion

Nighttime lights are able to detect the changes in human activities after earthquakes. In this study, we showed that though it is possible to see changes in the total nighttime light times series data as a result of an earthquake, there are changes in the time series that may be attributed to other factors not related to the earthquake. Therefore, we demonstrated the importance of decomposing a nighttime light time series into a trend and seasonal component in order to detect the changes in the nighttime light that are directly related to the effects of the earthquake. Change points were detected during the months of the earthquake events that were studied. Furthermore, we were able to show how the earthquakes change the trajectory of the trend component in some regions, and not in others, depending on the magnitude and damage the earthquake caused to the region.

However, there are two major limitations of using nighttime light imagery to monitor post-earthquake recovery of a region. First, cloud cover in the region results in missing values of the nighttime light imagery. In this paper, the simple interpolation method IDW was used to interpolate the missing values. However, given the simplicity of the method, significant error may have emerged. We were unable to obtain reference data to verify the interpolated values and resorted to using manual visual assessments for verification. Other more complicated interpolation methods such as kriging might be used to obtain better results but still, the inherent nature of the cloud cover in the images makes it very difficult to validate and quantify the errors of the interpolated values. Secondly, nighttime light imagery is more applicable for areas that are more urban with a relatively high normal nighttime light intensity. As seen in the 2016 Aceh earthquake, a region that is sparser in population, the nighttime light imagery detected a change point that, to our knowledge, does not correspond to any other events that could have possibly happened. Given these limitations, though nighttime lights imagery can provide a general overview of the recovery process post-earthquake, a combination of other higher resolution data sources is required to obtain a more detailed recovery assessment.

5. References

[1] D. Brown, S. Platt, and J. Bevington, *Disaster Recovery Indicators*. 2010.

[2] D. Brown *et al.*, "Monitoring and Evaluating Post-Disaster Recovery Using High-Resolution Satellite Imagery – Towards Standardised Indicators for Post-Disaster Recovery," *8th Int. Work. Remote Sens. Disaster Appl.*, no. March, p. 13, 2015.

[3] E. M. Rathje and B. J. Adams, "The Role of Remote Sensing in Earthquake Science and Engineering : Opportunities and Challenges," *Earthq. Spectra*, vol. 24, no. 2, pp. 471–492, 2008.
[4] L. Dong and J. Shan, "A comprehensive review of earthquake-induced building damage detection with remote sensing techniques," *ISPRS J. Photogramm. Remote Sens.*, vol. 84, pp. 85–99, 2013.
[5] C. Geiß and H. Taubenböck, "Remote sensing contributing to assess earthquake risk: From a literature review towards a roadmap," *Nat. Hazards*, vol. 68, no. 1, pp. 7–48, 2013.
[6] D. Brunner, G. Lemoine, and L. Bruzzone, "Earthquake damage assessment of buildings using VHR optical and SAR imagery," *IEEE Trans. Geosci. Remote Sens.*, vol. 48, no. 5, pp. 2403–2420, 2010.
[7] B. Adriano, J. Xia, G. Baier, N. Yokoya, and S. Koshimura, "Multi-Source Data Fusion Based on Ensemble Learning for Rapid Building Damage Mapping during the 2018 Sulawesi Earthquake and Tsunami in Palu, Indonesia," *Remote Sens.*, vol. 11, no. 7, p. 886, 2019.
[8] L. Moya, L. R. M. Perez, E. Mas, B. Adriano, S. Koshimura, and F. Yamazaki, "Novel unsupervised classification of collapsed buildings using satellite imagery, hazard scenarios and fragility functions," *Remote Sens.*, vol. 10, no. 2, 2018.
[9] L. Moya, E. Mas, B. Adriano, S. Koshimura, F. Yamazaki, and W. Liu, "An integrated method to extract collapsed buildings from satellite imagery, hazard distribution and fragility curves," *Int. J. Disaster Risk Reduct.*, vol. 31, no. October 2017, pp. 1374–1384, 2018.
[10] M. Chini, N. Pierdicca, and W. J. Emery, "Exploiting SAR and VHR optical images to quantify damage caused by the 2003 bam earthquake," *IEEE Trans. Geosci. Remote Sens.*, vol. 47, no. 1, pp. 145–152, 2009.
[11] Y. Dong, Q. Li, A. Dou, and X. Wang, "Extracting damages caused by the 2008 Ms 8.0 Wenchuan earthquake from SAR remote sensing data," *J. Asian Earth Sci.*, vol. 40, no. 4, pp. 907–914, 2011.
[12] P. Uprety and F. Yamazaki, "Use of high-resolution SAR intensity images for damage detection from the 2010 Haiti earthquake," *Int. Geosci. Remote Sens. Symp.*, vol. 2009, pp. 6829–6832, 2012.
[13] W. Liu, F. Yamazaki, H. Gokon, and S. I. Koshimura, "Extraction of tsunami-flooded areas and damaged buildings in the 2011 Tohoku-oki earthquake from TerraSAR-X intensity images," *Earthq. Spectra*, vol. 29, no. SUPPL.1, pp. 183–200, 2013.
[14] F. Yamazaki, W. Liu, and L. Moya, "Use of multitemporal lidar data to extract changes due to the 2016 Kumamoto earthquake," *Remote Sens. Technol. Appl. Urban Environ. II*, p. 15, 2017.
[15] F. Yamazaki and W. Liu, "Extraction of collapsed buildings due to the 2016 Kumamoto, Japan, earthquake using two-temporal Lidar data," no. October 2018, p. 25, 2018.
[16] S. Mavroulis *et al.*, "UAV and GIS based rapid earthquake-induced building damage assessment and application of the EMS-98 for the June 12, 2017 Mw 6.3 Lesvos (Northeastern Aegean, Greece) Abstract," 2018.
[17] D. Duarte, F. Nex, N. Kerle, and G. Vosselman, "Damage Detection on Building Facades Using Multi-Temporal Aerial Oblique Imagery," *ISPRS Ann. Photogramm. Remote Sens. Spat. Inf. Sci.*, vol. 4, no. 2/W5, pp. 29–36, 2019.
[18] Y. Li, W. Hu, H. Dong, and X. Zhang, "Building damage detection from post-event aerial imagery using single shot multibox detector," *Appl. Sci.*, vol. 9, no. 6, 2019.
[19] F. Nex, D. Duarte, A. Steenbeek, and N. Kerle, "Towards real-time building damage mapping with low-cost UAV solutions," *Remote Sens.*, vol. 11, no. 3, pp. 1–14, 2019.
[20] M. M. Bennett and L. C. Smith, "Advances in using multitemporal night-time lights satellite imagery to detect, estimate, and monitor socioeconomic dynamics," *Remote Sens. Environ.*, vol. 192, pp. 176–197, 2017.
[21] C. D. Elvidge, F. Hsu, K. E. Baugh, and T. Ghosh, "National Trends in Satellite-Observed Lighting," *Glob. Urban Monit. Assess. through Earth Obs.*, pp. 97–119, 2014.
[22] Q. Zhang and K. C. Seto, "Can night-time light data identify typologies of urbanization? A global assessment of successes and failures," *Remote Sens.*, vol. 5, no. 7, pp. 3476–3494, 2013.
[23] Y. Liu *et al.*, "Correlations between urbanization and vegetation degradation across the world's metropolises using DMSP/OLS nighttime light data," *Remote Sens.*, vol. 7, no. 2, pp. 2067–2088, 2015.
[24] M. O. Román and E. C. Stokes, "Holidays in lights: Tracking cultural patterns in demand for energy services," *Earth's Futur.*, vol. 3, no. 6, pp. 182–205, 2015.
[25] N. Levin, "The impact of seasonal changes on observed nighttime brightness from 2014 to 2015 monthly VIIRS DNB composites," *Remote Sens. Environ.*, vol. 193, pp. 150–164, 2017.
[26] X. Li, F. Chen, and X. Chen, "Satellite-observed nighttime light variation as evidence for global armed conflicts," *IEEE J. Sel. Top. Appl. Earth Obs. Remote Sens.*, vol. 6, no. 5, pp. 2302–2315, 2013.
[27] W. Jiang, G. He, T. Long, and H. Liu, "Ongoing conflict makes Yemen dark: From the perspective of nighttime light," *Remote Sens.*, vol. 9, no. 8, pp. 1–18, 2017.
[28] X. Li, C. Zhan, J. Tao, and L. Li, "Long-term monitoring of the impacts of disaster on human activity using

DMSP/OLS nighttime light data: A case study of the 2008 Wenchuan, China Earthquake," *Remote Sens.*, vol. 10, no. 4, pp. 1–17, 2018.

[29] X. Zhao *et al.*, "NPP-VIIRS DNB Daily Data in Natural Disaster Assessment: Evidence from Selected Case Studies," *Remote Sens.*, vol. 10, no. 10, p. 1526, 2018.

[30] X. Fan, G. Nie, Y. Deng, J. An, J. Zhou, and H. Li, "Rapid detection of earthquake damage areas using VIIRS nearly constant contrast night-time light data," *Int. J. Remote Sens.*, vol. 40, no. 5–6, pp. 2386–2409, 2019.

[31] X. Li, Z. Liu, X. Chen, and Q. Meng, "Assessment of the impact of the 2010 Haiti earthquake on human activity based on DMSP / OLS time series nighttime light data," vol. 13, no. 4, 2019.

[32] M. O. Román *et al.*, "NASA's Black Marble nighttime lights product suite," *Remote Sens. Environ.*, vol. 210, no. November 2017, pp. 113–143, 2018.

[33] Y. Cao, J. Zhang, M. Yang, and X. Lei, "Analysis of post-earthquake reconstruction for Wenchuan earthquake based on night-time light data from DMSP/OLS," *Ninth Int. Conf. Digit. Image Process. (ICDIP 2017)*, vol. 10420, no. July 2017, p. 104204W, 2017.

[34] C. D. Elvidge *et al.*, "The nightsat mission concept," *Int. J. Remote Sens.*, vol. 28, no. 12, pp. 2645–2670, 2007.

[35] C. D. Elvidge, K. E. Baugh, M. Zhizhin, and F.-C. Hsu, "Why VIIRS data are superior to DMSP for mapping nighttime lights," *Proc. Asia-Pacific Adv. Netw.*, vol. 35, no. 0, p. 62, 2013.

[36] K. Zhao *et al.*, "Detecting change-point, trend, and seasonality in satellite time series data to track abrupt changes and nonlinear dynamics: A Bayesian ensemble algorithm," *Remote Sens. Environ.*, vol. 232, no. April 2018, p. 111181, 2019.

[37] EOG Colorado School of Mines, "Version 1 VIIRS Day/Night Band Nighttime Lights." [Online]. Available: https://eogdata.mines.edu/download_dnb_composites.html. [Accessed: 21-Nov-2019].

[38] The Jakarta Post, "Central Sulawesi disasters killed 4,340 people, final count reveals." [Online]. Available: https://www.thejakartapost.com/news/2019/01/30/central-sulawesi-disasters-killed-4340-people-final-count-reveals.html. [Accessed: 21-Nov-2019].

[39] The Washington Post, "Indonesia: How the quake, tsunami and mud flows stunned experts." [Online]. Available: https://www.washingtonpost.com/world/asia_pacific/not-a-straightforward-event-how-multiples-disasters-stunned-experts-and-ravaged-a-corner-of-indonesia/2018/10/06/4394e20c-c967-11e8-b2b5-79270f9cce17_story.html. [Accessed: 21-Nov-2019].

[40] Liputan6, "Bupati: 30 Persen Wilayah Pidie Jaya Terdampak Gempa Aceh - News Liputan6.com." [Online]. Available: https://www.liputan6.com/news/read/2672206/bupati-30-persen-wilayah-pidie-jaya-terdampak-gempa-aceh. [Accessed: 21-Nov-2019].

[41] The Jakarta Post, "Aceh earthquake death toll reaches 35." [Online]. Available: https://www.thejakartapost.com/news/2013/07/05/aceh-earthquake-death-toll-reaches-35.html. [Accessed: 21-Nov-2019].

[42] X. Li, S. Liu, M. Jendryke, D. Li, and C. Wu, "Night-time light dynamics during the Iraqi CivilWar," *Remote Sens.*, vol. 10, no. 6, pp. 1–19, 2018.

[43] OpenStreetMap, "OpenStreetMap." [Online]. Available: https://www.openstreetmap.org. [Accessed: 21-Nov-2019].

[44] C. Daly, "Guidelines for assessing the suitability of spatial climate data sets," *Int. J. Climatol.*, vol. 26, no. 6, pp. 707–721, 2006.

[45] K. Zhao, D. Valle, S. Popescu, X. Zhang, and B. Mallick, "Hyperspectral remote sensing of plant biochemistry using Bayesian model averaging with variable and band selection," *Remote Sens. Environ.*, vol. 132, pp. 102–119, 2013.

